

Dear reviewer,

The reviewer's comments were highly insightful and enabled us to improve the quality of our manuscript. Our point by point responses to the each of the comments in the following pages. We hope that the revisions in the manuscript and our accompanying responses will be sufficient to make our manuscript suitable for publication in *Atmospheric Measurement Technique*.

Changes to the revised manuscript are shown in [blue](#).

10 We shall look forward to hearing from you at your earliest convenience.

Yours sincerely,

Professor Yong-Jun, Kim.

15

Address: School of Mechanical Engineering, Yonsei University, Seoul, Korea

Phone: +82-2-2123-7212

Fax: +82-2-312-2159

E-mail: [yjk@yonsei.ac.kr](mailto:yjk@yonsei.ac.kr)

20

# **OPEN DISCUSSION #1**

## **Question 1**

P1-18, I would not consider particle concentration of  $7000 \text{ cm}^{-3}$  as “high concentration” environment. The concentrations range from  $10^0 \text{ cm}^{-3}$  in clean environments to  $10^{6-7} \text{ cm}^{-3}$  in very polluted or industrial applications, so  $10^4 \text{ cm}^{-3}$  somewhere in the middle.

## **Answer 1**

We thank for your advice and agree with you. The number concentration range where the MEMS-based CPC can singly count particles was characterized as  $7.99 \sim 6850 \text{ cm}^{-3}$ . The high concentration in the original manuscript meant the upper concentration limit of our system, which was subjective term. Thus, we have deleted this term.

### **We modified the ‘Abstract’ of the revised manuscript as following,**

Our system measured the UFP number concentration with high accuracy (mean difference within 4.1 %), and the number concentration range where the proposed system can singly count particles was characterized as  $7.99\text{--}6850 \text{ cm}^{-3}$ . Thus, the proposed system has a potential of being used for UFP monitoring in various environments (e.g., air filtration system, high-precision industries utilizing cleanrooms, indoor/outdoor atmospheres).

## **Question 2**

P1 120-25, There are various sources of UFPs, such as secondary particle formation in the atmosphere from the existing gases. Also their fraction of the total concentration is highly specific to the environment, or measurement time.

## **Answer 2**

We thank for your advice and letting us improve the solidity of the manuscript. We have modified the text on the sources of UFPs in the revised manuscript, referring to the newly-added references.

### **We modified the 1<sup>st</sup> paragraph of ‘Introduction’ in the revised manuscript as following,**

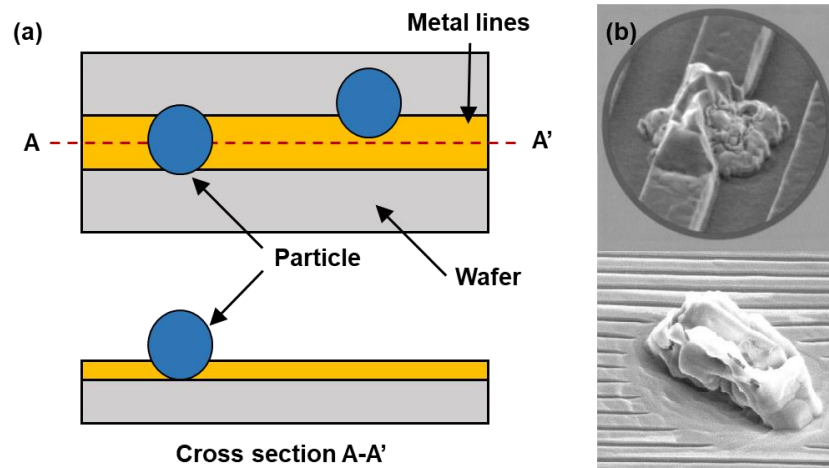
Monitoring of airborne ultrafine particles (UFPs), which are smaller than 100 nm, is needed in various fields for human health and yield enhancement in industrial fields (Donaldson et al., 1998; Donovan et al., 1985; Hristozov and Malsch, 2009; Li et al., 2016; Liu et al., 2015). While they have a variety of anthropogenic and natural sources, in urban area, UFPs are largely generated from the vehicle exhaust (e.g., soot agglomerates, secondary particles from hazardous gaseous precursors) (Kim et al., 2011; Kittelson, 1998; Shi et al., 1999). Moreover, because of dramatic developments in nanotechnology, engineered UFPs for commercial and research purposes have been produced at a large scale. These incidentally and intentionally generated UFPs are more harmful to human health than larger counterparts: UFPs have a higher chance to deposit in the lower respiratory system and are more toxic owing to their larger surface-to-volume ratios, which causes oxidative stress, pulmonary inflammation, and tumor development (Hesterberg et al., 2012; Hext, 1994; Li et al., 2003; Renwick et al., 2004). Thus, onsite monitoring is needed to assess and minimize UFP exposure.

### Question 3

P1 129-30, “High-precision industries with cleanrooms also need UFP monitoring to increase the production yield”, what does this mean? How is UFP and production yield connected?

### Answer 3

5            Currently, semiconductor devices are being processed at the linewidth of a few nanometers. Thus, the related manufacturing process requires an extremely clean environment to prevent contamination. Although the air-purification system with ultra-low particulate (ULPA) filter eliminate the contaminants of the air entering the clean room, it cannot control the internally-generated UFPs the manufacturing instruments under operation (e.g., chemical vapor deposition (CVD), metallization, wet etching). As shown in Figure R1, these UFPs can be attached to wafers during the manufacturing process. If they are deposited on electrodes of a chip, they cause the interruption of the current flow, making the whole chip unusable and thereby reducing the yield of the semiconductor device. In this regard, ISO 14644-12, “Cleanroom and associated controlled environment: Specifications for monitoring air cleanliness by nanoscale particle concentration”, has been developed to guide how to monitor UFPs in cleanrooms.



15 Figure R1: (a) the schematic view and (b) SEM images of UFP deposition on a wafer.

**We modified the 1<sup>st</sup> paragraph of ‘Introduction’ in the revised manuscript as following.**

High-precision industries with cleanrooms also need UFP monitoring to increase the production yield. For instance, in case of the semiconductor industry, as the minimum feature size of the semiconductor devices approaches to 7 nm, particles with the diameter of a few nanometers are critical (Neisser and Wurm, 2015). Although the air-purification system equipped with ultra-low particulate (ULPA) filter eliminate the contaminants in the air entering the clean room, it cannot control the internally-generated UFPs during the manufacturing processes (e.g., chemical vapor deposition (CVD), metallization, wet etching) (Choi et al., 2015; Manodori and Benedetti, 2009). If they are deposited on electrodes of a chip, they cause the interruption of the current flow, making the whole chip unusable and thereby reducing the yield of the semiconductor device (Libman et al., 2015). In this regard, ISO 14644-12 has been recently developed to guide how to monitor UFPs in cleanrooms.

### Question 4

P1 134-36, Why does it need to be portable or low-cost? Any “normal” CPC will give the same information.

## Answer 4

You have raised an important point. Compared to commercial CPCs, the major advantages of the proposed system are compactness and cost efficiency, making us actively utilize it for on-site monitoring applications.

The typical CPCs (model 3025, TSI Inc., USA), which provide the accurate number concentration of UFPs as small as 3 nm, are mainly used for academic research due to their high cost and large size. Although, to my knowledge, the smallest portable CPC with the lower detectable size of 10 nm is currently in the market (model 3007, TSI Inc., USA), it is still considered bulky (292 mm × 140 mm × 140 mm) and expensive for the ownership (~ \$ 10,000). In the contrast, the proposed system is far smaller and cheaper than even the portable CPC without the significant performance degradation (minimum detectable size: 12.9 nm).

The compactness and cost-efficiency of CPCs are preferred when monitoring in real-world environments where spatial and temporal variations of UFP concentration are enormous. For example, in urban areas, the sources of UFPs are highly localized and their migration patterns driven by air-flow are very complex, because skyscrapers, people and traffic are highly concentrated. Also, in cleanrooms, since a majority of UFPs are mainly generated from the manufacturing instruments under operations, their sources are also localized. Thus, it is required to establish simultaneous monitoring at multiple points or dense monitoring networks for measuring these environments. The proposed system has a potential of being an appropriate solution for these applications, because each sensing node must be not only accurate, but also compact and inexpensive.

**We modified the 1<sup>st</sup> paragraph of 'Introduction' in the revised manuscript as following,**

In order to monitor the concentration field of UFPs in these environments where the spatial and temporal variations of UFP concentrations are enormous, a portable and low-cost sensors are required to establish simultaneous monitoring at multiple points or establish dense monitoring networks.

## Question 5

P2 11-2, "because they are theoretically capable of counting every single UFP", this could be reformulated a little bit. Why e.g. your CPC is limited to concentration around 7000 cm<sup>-3</sup> or smallest size of 13 nm? Same theoretical limitations apply for other CPC designs, just resulting in different limiting numbers.

## Answer 5

We thank for your advice and agree with you. Any confusing sentence in the manuscript must be corrected. The sentence, "they are theoretically capable of counting every single UFP", will be reformulated as they are capable of counting individual particles."

**We modified the 2<sup>nd</sup> paragraph of 'Introduction' in the revised manuscript as following,**

Condensation particle counters (CPCs) are one of the most widely used UFP detection instruments and are based on the heterogeneous particle condensation technique. They grow UFPs to micro-sized droplets through condensation and count them by optical means. Compared to an electrical method (measuring the number concentration of UFPs by electrically charging them and sensing their current), CPCs provide extremely sensitive and precise counting because they are capable of counting individual particles.

## Question 6

P2 I3-4, “64 size channels per decade”, from where this number is obtained? With a DMA you can in practice select almost infinite number of size channels

## Answer 6

5 We thank for your advice. The DMA can select almost infinite number of size channels by adjusting its classification voltages. 64 size channel per decades means that the commercially-available scanning mobility particle sizer (SMPS) typically perform monitoring of UFP size distribution with a resolution of 64 channels per decade. However, since this phrase is confusing and the number of size channels of SMPS is not established, the ‘64 size channel per decades’ terms will be deleted in the revised manuscript.

10

**We modified ‘Description of the MEMS-based CPC’ part of the [revised manuscript](#) as following,**

Moreover, if a differential mobility analyzer (DMA) is used as a particle size selector, CPCs can offer higher particle size resolution than any other particle-sizing instruments (Sioutas, 1999; Stolzenburg et al., 2017).

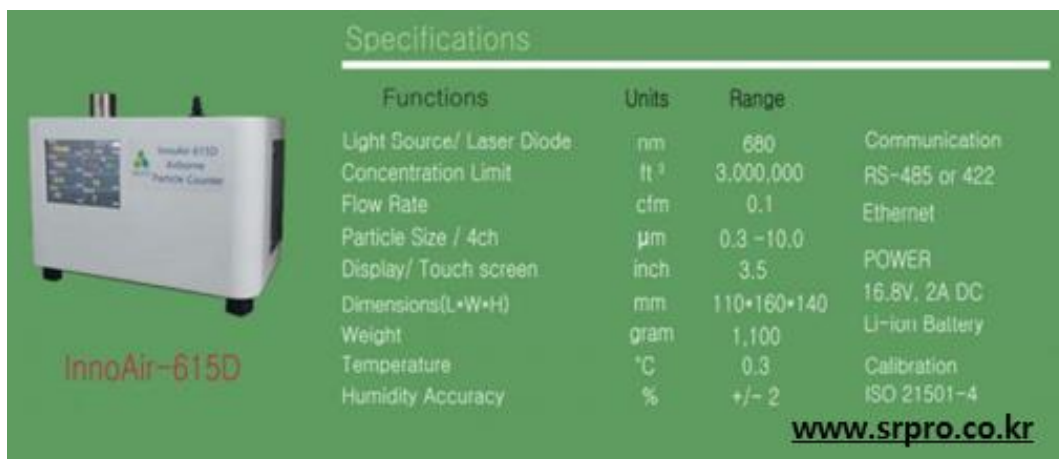
## Question 7

15 P2 L39, is the OPC also homemade or commercially available?

## Answer 7

We thank for your advice. Although the main argument of the manuscript is the chip-sized particle growth chip, there is little information about the detector.

20 The optical detector used in the proposed system is a detection part of the commercial optical particle counter (Innoair-615D, Innociple Co., KR) which is capable of counting individual particles larger than 0.3  $\mu\text{m}$  (Figure R2).



The image shows a photograph of the InnoAir-615D Airborne Particle Counter on the left and a table of its specifications on the right. The device is a white rectangular box with a small screen and several ports on top. The table lists various functions, units, and ranges for the device.

Functions	Units	Range	
Light Source/ Laser Diode	nm	680	Communication
Concentration Limit	ft <sup>3</sup>	3,000,000	RS-485 or 422
Flow Rate	cfm	0.1	Ethernet
Particle Size / 4ch	$\mu\text{m}$	0.3 -10.0	POWER
Display/ Touch screen	inch	3.5	16.8V, 2A DC
Dimensions(L*W*H)	mm	110*160*140	Li-ion Battery
Weight	gram	1,100	Calibration
Temperature	$^{\circ}\text{C}$	0.3	ISO 21501-4
Humidity Accuracy	%	+/- 2	

[www.srpro.co.kr](http://www.srpro.co.kr)

Figure R2: The specification of the commercial optical particle counter. Its detection part was used in this study.

25 Figure R3 shows the (a) exploded view, (b) section A-A' and (c) section B-B' of the optical detector. It consists of the sensing chamber and optics (laser, cylindrical lens, elliptic mirror, photodiode, light trap). Introduced droplets are firstly arranged in a row in the acceleration nozzle (i.e., the outlet of the particle growth chip) and enter the sensing chamber.

The droplets then pass through the place where the condensed thin beam is irradiated. The mirror collects the scattered light from a droplet and redirect it to the photodiode.

When the laser beam passes through the cylindrical lens, the shape of the laser beam at the focal point is not a point but a very thin surface. In addition, the acceleration nozzle at the chip outlet is only 0.8 mm in diameter and is located about 1.5 mm below the point where the beam passes. Therefore, as shown in Figure R3 (c), on the condition that the coincidence error does not occur (when two particles do not pass through the viewing volume at the same time), almost all the grown micro-droplets are counted in the optical detector.

In the perspectives of the structure and detection principle, the optical detector used in this study is similar to the high-precision OPC rather than dust sensors. Thus the proposed system demonstrated particle counting performance, which was comparable to those of the reference CPC (model 3772, TSI Inc., USA).

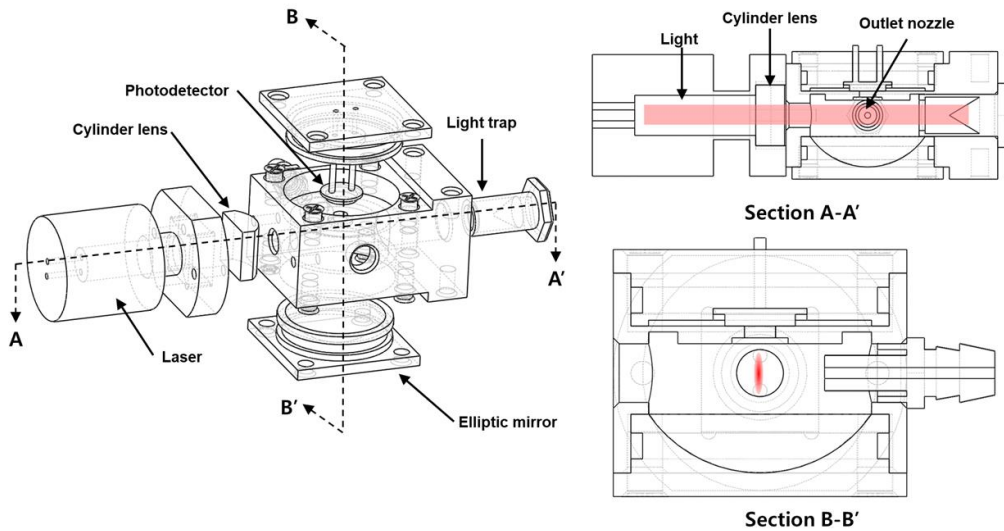


Figure R3: The (a) exploded view, (b) section A-A' and (c) section B-B' of the optical detector used in this study.

**We added the description of the optical detector in '2 Description of the MEMS-based CPC' of the revised manuscript as following.**

~. The maximum Reynolds number in the channel at the given flow rate was only 32, which means that the sample stream in the channel was in the fully laminar regime.

The detection part of the commercial optical particle counter (OPC; Innoair-615D, Innociple Co., KR), which provided the time resolution of 6 s, was used as the optical detector in the proposed system. It consists of the sensing chamber and optics (laser, cylindrical lens, elliptic mirror, photodiode, light trap). Introduced droplets are firstly arranged in a row in the acceleration nozzle (i.e., the outlet of the particle growth chip) and enter the sensing chamber. The droplets then pass through the place where the condensed thin beam is irradiated. The mirror directs the scattered light of a droplet to the sensing surface of the photodiode. When the laser beam passes through the cylindrical lens, the shape of the laser beam at the focal point is not a point but a very thin surface. In addition, the acceleration nozzle at the chip outlet is only 0.8 mm in diameter and is located about 1.5 mm below the point where the beam passes. Therefore, on the condition that the coincidence error does not occur (the two particles do not pass through the viewing volume at the same time), almost all the grown micro-droplets are counted in the optical detector.

## Question 8

P4 115-17, what is the difference between TSI Co. Ltd. and TSI Inc.?

## Answer 8

We thank for letting us catch the mistakes in our manuscript. TSI Co. Ltd. and TSI Inc. are the same company. In the revised manuscript, we will unify with TSI Inc.

### 5 We modified '4 Experimental setup' of the revised manuscript as following,

10 They were electrically charged by a soft X-ray charger (XRC-05, HCT Co., KR) and then classified to a specific diameter with two types of DMA: (1) nano DMA (model 3085, TSI Co. Ltd., USA) for particles in the size range from 3 to 10 nm, (2) long DMA (model 3081A, TSI Co. Ltd., USA) for particles in the size range from 5 to 140 nm. Next, the number concentration of the monodisperse Ag particles were controlled ( $0\text{--}24000\text{ N cm}^{-3}$ ) in the dilution bridge system by adjustment of the needle valve. Finally, the concentration-controlled and monodisperse Ag particles were introduced into the proposed system and reference instrument, which was either a CPC (model 3772, TSI Inc., USA) or aerosol electrometer (model 3068B, TSI Inc., USA).

## Question 9

15 Section 5.1, it is not evident whether there was a flow above the butanol surface when the dry-out region was measured. If not, does the flow have any effect on the dry-out region formation?

## Answer 9

We described the flow condition and modified in '5.1 Working fluid transmission and evaporation' of the revised manuscript as following,

20 In order to obtain optical images of the dry-out region formation, a single glass slide with the patterned electrodes and micropillar array was used. For this reason, there was no flow rate during the experiment. Although, due to the advection, the flow rate has effect on the area of the dry-out region to some extent, the vapor pressure at which the dry out region started to form (164.1 mmHg at 80 °C) was 8.7 times larger than the designed value of the saturator (18.9 mmHg at 40 °C). Thus, although there was no flow above the butanol surface when measuring the dry-out region, the dry-out region  
25 didn't occur in the saturator of the MEMS-based CPC under operating condition.

## Question 10

P5 117-20, reformulate the sentences, partly badly written, partly ambiguous. "Initially" refers to A happening before B.

30 P5 123, I would say non-negligible. If the Kelvin diameter is 2.45 nm, how come 90 % of particles are detected only at 20 nm? The experimental characterization of the CPC is adequate, while the authors do not consider carefully enough why the cut-off is 13 nm. For example, according to its manual, TSI 3775 has temperatures of 39C in the saturator and 14C in the condenser, compared to 40C and 10C in the MEMS CPC. With smaller dT, the cut-off of the 3775 is 4 nm, while the MEMS CPC cut-off is 13 nm. TSI 3772 has cut-off of 10 nm at dT of 17C. How come? Even the Kelvin diameter inside the MEMS CPC is calculated to be 2.45 nm. Satisfactory explanation for this should include discussion  
35 and/or experiments and/or modeling of particle losses inside the CPC, the capability of the saturator to fully saturate the flow, and the condenser supersaturation profile. This should help to understand why the cut-off is 13 nm and not 2.45 nm

what the Kelvin diameter predicts. Indeed, in careful experiments it has been found that the Kelvin diameter overestimates observed the cut-off, e.g. Iida et al. (2009) and Winkler et al. (2008).

The next sentence is ambiguous, what is the supersaturation that you calculate the Kelvin diameter? There is a supersaturation profile in the condenser, so single value for the Kelvin diameter is not good, unless it is a particle trajectory weighted average or something similar. P5 117-20, 5 and 9 nm are quite much above the calculated Kelvin diameter, so why at 9 nm it increases sharply and not above 5 nm?

### Answer 10-1

We thank for letting us know the ambiguity of the original manuscript.

**We have modified the sentence in ‘5.3 Size-dependent particle counting efficiency’ of the revised manuscript on as followings.**

Figure 7 shows the size-dependent counting efficiency of the MEMS-based CPC. The size range of Ag particles was controlled concentration range to 1000-2000 N cm<sup>-3</sup>. The sampling times for each data point were 300 s, and the measurement uncertainty based on the Poisson statistics was 0.02 %. It was found that the proposed system detected 1 % of UFPs with the size of 5 nm, and the detection efficiency increased sharply above 9 nm.

### Answer 10-2

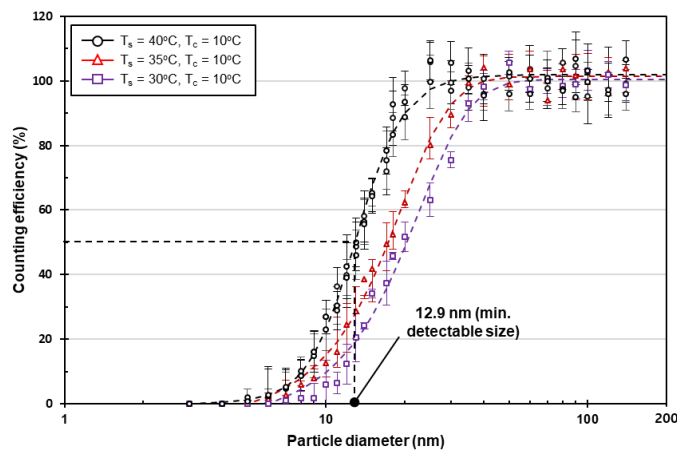


Figure 7: Particle counting efficiency of the MEMS-based CPC as a function of the particle size and saturator temperature. The particle size at which the particle counting efficiency was fitted to 50 % was 12.9 nm ( $T_s = 40^\circ\text{C}$ ), 17.3 ( $T_s = 35^\circ\text{C}$ ) and 20.4 ( $T_s = 30^\circ\text{C}$ ), respectively.

The particle loss of our system was characterized using the counting efficiency, since it is defined as the efficiency of the system at detecting the introduced particles, and thereby describes the overall transportation/activation efficiencies. To accurately measuring the counting efficiency, the following procedures were carried out to verify that particles with the same concentration were introduced into the two systems. First, to minimize the particle loss induced from the turbulence at the bifurcation, a flow splitter with a very small angle of cleavage (model 3708, TSI Inc., USA) was used. The tubes which leads from the flow splitter to the both systems were electrostatic dissipative to minimize the electrostatic particle loss, and their lengths were carefully adjusted to match the transportation times. To verify that the particles which introduced into both systems have the same concentrations, it was confirmed that the counting efficiency was close to 100 % when particles with size of 100 nm were introduced (it was assumed that they were activated and grew into droplets with 100 % efficiency). Then, while reducing the size of the introduced particles to 40 nm by adjusting the voltages of a



DMA, it was confirmed whether the counting efficiency remained constant. Through these procedures, it was verified that the concentrations of the particles delivered to the two systems were the same. The size-dependent counting efficiency of the proposed system was further characterized using Ag particles in the size range of 3 to 140 nm (Figure 7). Particles with size of 140 nm were almost the maximum size that the Ag particle generator (EP-NGS20, EcoPictures, Co. KR) could generate. The number concentration range of the Ag particles was controlled to be 1000–2000 N cm<sup>-3</sup>. Although there are small fluctuations, the counting efficiency of the particles larger than 25 nm was nearly close to 100 % (T<sub>s</sub> = 40°C). It was close to 100 % and constant in the size range from 25 to 140 nm, indicating that the internal particle loss in this size range was negligible.

As the reviewer's advice, since the saturation ratio is the highest at the centreline in the condenser and close to 1 on the wall, the Kelvin diameter should be expressed as the profile in the condenser channel section rather than a single value. However, unfortunately, we did not have CFD software available to characterize the Kelvin distribution at present. Saturation ratio was calculated using butanol saturation vapor pressures at the wall temperatures of the saturator and condenser. The Kelvin diameter was obtained based on this value, which were seemed to be small value, because the temperature at the centreline of the condenser channel was higher than the wall temperature. Nonetheless, the reason why the minimum detectable size was relatively high for the given temperature difference can be explained. Since the saturator and condenser were close to each other and thereby have thermal interference, the condenser temperature might be higher than its originally-designed value due to the heat transfer from the saturator to the condenser. It is expected that this problem can be solved by increasing the thickness of the thermal barrier between the saturator and condenser.

**We modified '5.3 Size-dependent particle counting efficiency' of the revised manuscript as following,**

Figure 7 shows the size-dependent counting efficiency of the MEMS-based CPC. The size range of Ag particles was controlled concentration range to 1000-2000 N cm<sup>-3</sup>. The sampling times for each data point were 300 s, and the measurement uncertainty based on the Poisson statistics was 0.02 %. To evaluate the effect of the temperature difference, the counting efficiency was characterized when the condenser temperature (T<sub>c</sub>) was 10 °C and the saturator temperatures (T<sub>s</sub>) were 30, 35 and 40 °C. At 40 °C (the design value of the saturator temperature), the same experiments were repeated three times to confirm the measurement reliability. When the saturator temperature was 40 °C, it was found that our system detected 1 % of UFPs with the size of 5 nm, and the detection efficiency increased sharply above 9 nm. This was primarily because the activation efficiency ( $\eta_{act}$ ) increased when the particle size exceeded the Kelvin diameter (2.34 nm). The transport efficiency ( $\eta_{trans}$ ) also increased, because the diffusivity of a particle decreases with the increment of the particle size. The counting efficiency data were curve-fitted using

$$\eta_d = \alpha + \frac{(\beta - \alpha)}{1 + (d_p/\gamma)^\delta}, \quad (3)$$

where  $\alpha$ ,  $\beta$ ,  $\gamma$  and  $\delta$  are fitting constants of 101.96, 2.00, 12.99 and 4.70, respectively. The corresponding minimum detectable size is defined as the size at which particles are detected with 50 % efficiency and was found to be 12.9 nm. The detection efficiency was 90 % at 20.1 nm and reached 95 % at 22.9 nm. It was close to 100 % and constant in the size range from 25 to 140 nm, indicating that the internal particle loss in this size range was negligible.

The minimum detectable size was relatively higher than that of the commercial CPC operating at the same temperature difference. Since the saturator and condenser were close to each other and thereby have thermal interference, the condenser temperature might be higher than its originally-designed value due to the heat transfer from the saturator to the condenser. It is expected that this problem can be solved by increasing the thickness of the thermal barrier between the saturator and condenser.

## Question 11

P5 I30, please indicate the background count rate also in units of count every x seconds. If these background counts are originating from homogeneous nucleation, it should already hint you why the cut-off of your CPC is so far away from the Kelvin diameter.

## 5 Answer 11

We thank for your pointing. We modified '5.4 Detectable concentration range' of the revised manuscript as following,

When the temperature difference between the saturator and condenser was set to 30 °C, the average number concentration and counting rate during the measurement period (background concentration) was 0.05 N cm<sup>-3</sup> and 0.125 N s<sup>-1</sup>, respectively, indicating that homogeneous nucleation hardly occurred.

## Question 12

P5 I32-P6 I6, does the concentration ratio CPC/AEM plateau immediately above concentrations of 7000 cm<sup>-3</sup>? With some corrections the CPC is possibly usable also at concentrations higher than 7000 cm<sup>-3</sup>.

## Answer 12

15 You have raised an important point. Even if the number concentration is higher than the upper limit of the proposed system, it can be measured through calibration using curve fitting or nephelometric technique.

The proposed system was compared with an aerosol electrometer at a UFPs number concentration of 0 to 24000 N cm<sup>-3</sup>. Figure 8 shows (a) the time series of number concentrations measured with the proposed system and an aerosol electrometer and (b) a one-to-one comparison of the measured number concentrations by both systems. When the UFP number concentration exceeded 7000 N cm<sup>-3</sup>, the difference in the number concentration of the proposed system and the aerosol electrometer gradually increased. When the concentration exceeded 6852 N cm<sup>-3</sup>, the logarithmic function was well fitted to the response curve of the proposed system, as expressed in Figure 8b. In case that the calibration was applied to the proposed system, the average difference between both systems was only 2.8 %.

25 We modified 'Figure 8' of the revised manuscript as followings,

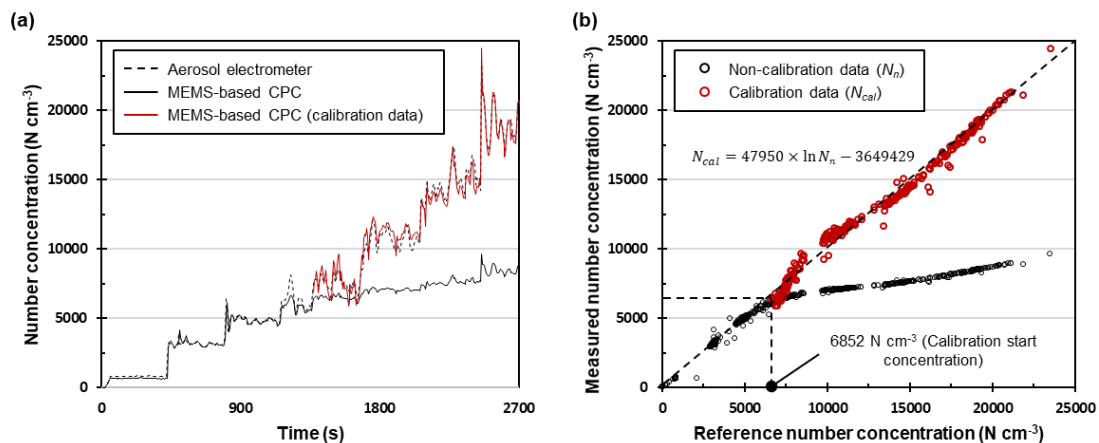


Figure 8: (a) Time series of the number concentrations with the MEMS-based CPC and aerosol electrometer; (b) one-to-one comparison of the measured number concentrations for both systems.

We discussed the measurement accuracy in high concentration in ‘5.4 Detectable concentration range’ of the revised manuscript as followings,

Thus, in case of the concentration exceeded  $6852 \text{ N cm}^{-3}$ , the logarithmic function was fitted to the response curve of the proposed system, as expressed in Figure 8b. When the calibration based on the fitted curve was applied to the proposed system, the average difference between both systems was within 2.8 %.

### Question 13

P6 110, why averaging of 6s? is the CPC performance comparable at 1s resolution?

### Answer 13

The reason why the data was averaged over 6 s was that the purchased OPC, which was used for calibration, provided the options of 6s, 30s and 1 min resolution. If it operates at 1 s resolution, it is expected that the measurement uncertainty induced from Poisson statistics will be increased.

We added the time resolution of the miniature OPC in ‘2 Description of the MEMS-based CPC’ of the revised manuscript on page x as followings,

The detection part of the commercial optical particle counter (OPC; Innoair-615D, Innociple Co., KR), which provided the time resolution of 6 s, was used as the optical detector in the proposed system.

### Question 14

Some claims are made on the cost-effectiveness of the CPC, which, however, should be considered carefully until the CPC is actually sold, as the final price of the CPC depends on many things, which are not discussed here, such as production volumes, company structure etc. Possibly material costs can be compared if you get that information from other manufacturers, which I doubt. Indeed, I believe this manufacturing method can possibly be cheaper than the current designs, while the current manuscript does not support that with numbers.

I believe this manufacturing method can possibly be cheaper than the current designs, while the current manuscript does not support that with numbers. P6 122, what is the price of your CPC? Or manufacturing price (materials or materials + work) compared to manufacturing price of some other commercial CPC? I would be careful in making claims about cost-effectiveness without these numbers.

### Answer 14

Although it is necessary to determine the actual price of the proposed system, please understand that, since we are a graduate laboratory, it is difficult to calculate its exact price with numbers. The reason is that all the materials used in the proposed system were purchased at a retail price with minimum quantity and therefore relatively expensive. In addition, the MEMS process is based on a batch process, it has a great advantage in mass production. Therefore, in the present situation where its demo version has been just developed, it is difficult to calculate the accurate price including the depreciation cost of manufacturing equipment and labor cost, or considering the effect of company structure. Also, it is

difficult to compare the price of the proposed system with that of commercial CPC because of the limited information about specific material + work put into the production of commercial CPCs.

The main argument of this paper is the production of low-cost particle growth unit using MEMS technology. Therefore, in this paper, the materials used in the MEMS-based particle growth system will be listed in the supplemental information, and model number and manufacturer of other components (e.g., pumps, flow meters) will be specified in the revised manuscript.

**We added the component and price information in the supplemental information as followings.**

The materials used for the MEMS-based particle growth system are summarized in Table S1.

Table S1: Material used for manufacturing a single MEMS-based particle growth system.

Components	Used material	Manufacturer	Retail price	Used quantity	Price (\$)
3D printed channel	SLA (Stereolithography Apparatus)	3D MON, KR	10 \$ / EA	1	10
Glass	Sodalime glass	SEMISTORE, KR	3 \$ / EA	2 EA	6
Integrated glass slide	electrodes	AZ GXR-601 Photoresist	420 \$ / 3.8 L	5 ml	0.55
		MIF-300 developer	170 \$ / 20 L	200 ml	1.7
Micropillar wick		SU-8 2100 photoresist	840 \$ / 500 ml	5 ml	8.4
		SU-8 developer	336 \$ / 3.8 L	100 ml	8.8

### Question 15

P6 I23, 91.5% of what? Price, weight, volume?

### Answer 15

**We modified ‘Conclusion’ part of the revised manuscript on page 6 as following,**

In terms of compactness and cost-efficiency, the proposed system is superior to conventional instruments. The physical volume of the proposed system is only 8.5 % of the volume of the commercially-available portable CPC (e.g., model 3007, TSI Inc., USA).

### Question 16

Fig1, something missing from Air inlet

Fig4, why in the picture of aerosol electrometer reads condensation particle counter, and in the reference CPC reads electrometer?

### Answer 16

**Thank you for letting us know. We modified ‘Figure 1’ in the revised manuscript as following,**

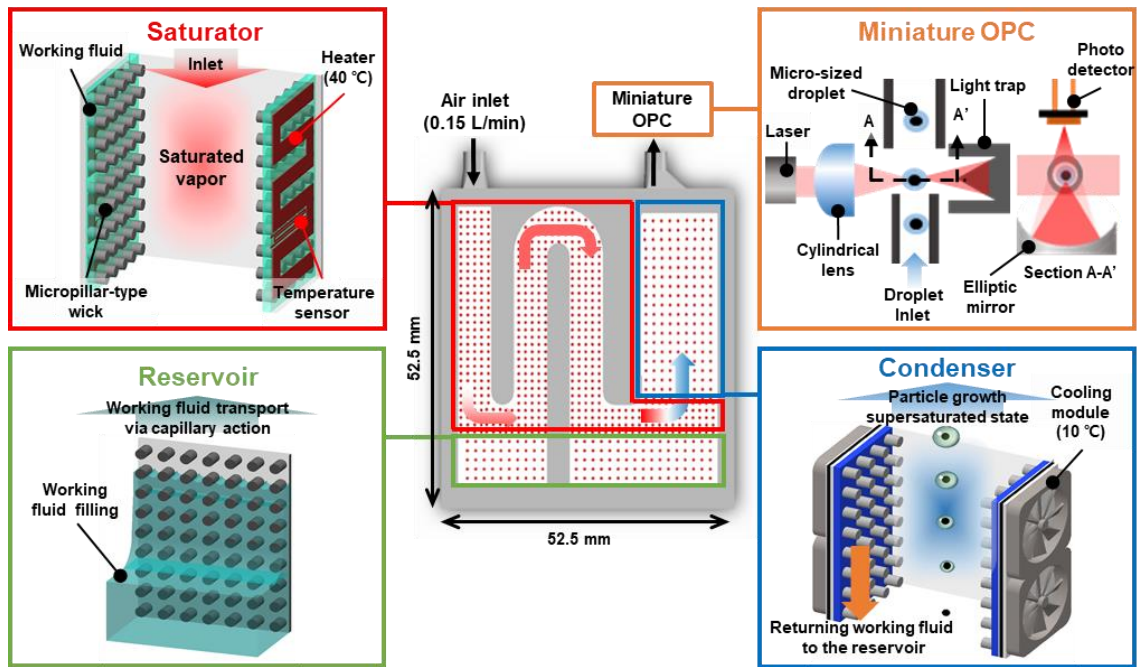


Figure 1: Schematic illustration of the MEMS-based CPC. The proposed system consists of four parts: the reservoir, saturator, condenser, and miniature OPC. The reservoir supplies the working fluid to the saturator via capillary action by the micropillar-type wick. The saturator heats the working fluid to generate saturated vapor. The saturated air becomes supersaturated when cooled by the condenser. UFPs grow into micro-sized droplets in the condenser and are counted by the miniature OPC.

5

**We modified ‘Figure 4’ in the revised manuscript as following.**

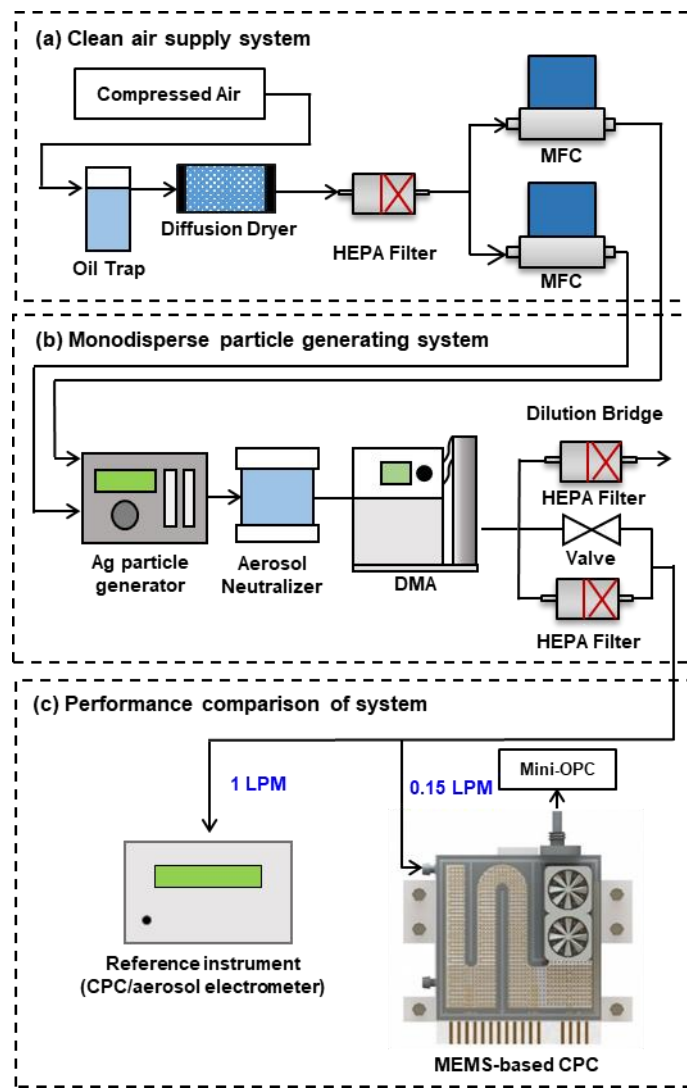


Figure 4: Schematic of the experimental setup for evaluating the performance of the MEMS-based CPC.